

THE 4TH INTERNATIONAL CONFERENCE ON ALUMINUM ALLOYS

MODERN MICROSTRUCTURAL ANALYSIS OF ALUMINUM ALLOYS

D. B. Williams

Lehigh University, Department of Materials Science and Engineering, Whitaker Laboratory,
5 East Packer Avenue, Bethlehem PA 18015-3195, USA

Abstract

Over the last forty years, the understanding and control of the properties of aluminum alloys has progressed primarily through the development of techniques that provide an ever-more complete characterization of the microstructure and microchemistry of the alloys. The principal and most versatile tool for this characterization has been the transmission electron microscope (TEM) which has developed to the point where it can provide images, diffraction patterns and elemental information from the micrometer to the sub-nanometer scale. In this review, various examples will be given of the application of TEM techniques to the study of Al alloys, with emphasis on simple binary and ternary systems which are often the model for more complex multi-component commercial alloys. In all cases the examples will highlight the information that the microscopy provides pertinent to the properties of the alloys themselves, such as the precipitation behavior, the phase diagram, dislocation-precipitate interactions and interfacial segregation.

Introduction

Aluminum alloys are perhaps the best suited of all commercial materials for study in the TEM. The reasons behind this statement are as follows. First, the average atomic number (Z) of the alloys is low - approximately that of pure Al, since the total amount of alloying elements is usually less than 10%. This low Z means that at typical TEM accelerating voltages (~100 kV) the electron beam can penetrate through substantial thicknesses of material. Consequently, making the thinnest specimens is not always so critical and in these circumstances, interpretation of the microstructure need not be complicated by thin foil sectioning effects. Thus, it is easier to relate thin foil observations to the behavior of the bulk material. Second, in cases where high quality, very thin foils are required, specimen preparation of Al alloys *per se* is generally very easy. Most Al alloys can be easily and rapidly thinned to electron transparency using simple electropolishing techniques that, with care, provide an excellent surface finish and result in minimal introduction of specimen preparation artifacts. Solutions of 10-20% perchloric or nitric acids in ethanol or methanol at -30°C are almost universal thinning media for Al alloys. Such easy preparation was one of the reasons why Al alloys were amongst the first materials to be studied in the mid-1950s when thin foil techniques were developed by Hirsch and co-workers in the U.K. Indeed, the first observation of dislocations moving in a metal were made in an Al alloy, and these pictures [1], constitute an historic part of the development of electron microscopy of materials given the preceding period of controversy over the very existence of dislocations. Third, because of the tendency of Al alloys to develop a very thin, protective oxide film, TEM thin foils remain pristine for long periods of time after preparation, making long term, routine, reproducible study of the alloys very straightforward. Fourth, if very thin specimens can be made, the electron beam does not spread very much on passing through the foil, thus providing very high spatial resolution for atomic level imaging and for elemental analysis.

These various advantages are often further helped by the alloying of Al with still lighter elements such as Mg and Li, and indeed many of the examples in this article come from Al-Li alloys, both because of the author's many years of study of this particular system, and the intense interest from the aluminum manufacturers and aerospace industry users in developing these alloys. Conversely, these very advantages pose difficulties in studying Al alloys with other modern microstructural and microanalytical techniques. For example, it proved extremely difficult to create Al needles for atom probe/field ion microscopy (AP/FIM) studies because the needles would deform under the high stress field at the tip, due to the ease of dislocation motion. The Al surface oxide also required in-situ cleaning in ultra-high vacuum if the oxide alone was not to be imaged. This same factor has meant that very limited studies have been carried out with such surface-sensitive techniques as scanning tunneling microscopy, atomic force microscopy, scanning ion microscopy and high resolution scanning electron microscopy. In fact in a recent comprehensive volume on the structure and properties of Al alloys [2], almost every figure in the text was either a light micrograph or a TEM image. A single FIM micrograph was present and a few low resolution SEM images of fracture surfaces. Thus, it is quite appropriate in the context of a conference on Al alloys to emphasize TEM as the pre-eminent modern microstructural technique used almost exclusively by researchers in the field.

All of the advantages described above contributed to the fact that Al alloys were amongst the first materials to be investigated by TEM techniques as they developed. By way of introduction to the pervasive nature of the TEM in the study of Al alloys it is worth noting some of the following:- For example, the classical studies of the nature of precipitate-matrix interfaces were carried out by Nicholson and co-workers in the 1960s (e.g. [3]) leading to our understanding of the critical importance of the interface coherency in the mechanical properties of precipitation-hardened alloys. The first high resolution studies of GP zones in Al-Cu alloys were carried out by Philips [4], in the early 1970s, further aiding our understanding of the metastable precipitation sequences that control the mechanical properties of all commercial Al alloys. Much of the early evidence for homogeneous, heterogeneous nucleation and spinodal decomposition arose from combined TEM imaging and diffraction studies (see Porter and Easterling [5] for a textbook summary of this area). Early elemental segregation studies using analytical electron microscopy (AEM) techniques also revealed the phenomena of grain boundary segregation of solute elements, accounting for precipitate-free zone formation. This was achieved through the application of x-ray microanalysis in the electron microscope microanalyzer [6]. In a similar vein, segregation accompanying precipitation was amongst the first materials problem to be analyzed in the early days of electron energy-loss spectrometry in the TEM [7]. In this review it is not possible to give a comprehensive listing of all the publications in which Al alloy characteristics have been discerned via TEM. Instead a sampling of the literature will be given emphasizing both the importance of the individual TEM techniques and illustrating the pivotal role of TEM in understanding many of the important properties of Al alloys.

These pioneering studies in Al alloys often opened the way for the application of TEM techniques to other important alloy systems such as Ni-base superalloys, high strength low alloy steels and the more recent developments in transformation toughened ceramics and metal-semiconductor interfaces. Similarly, as new microstructural analysis techniques have arrived, such as the various forms of scanning microscopy (electron, ion, acoustic, tunneling etc.) the contributions made by these newer techniques have, in many cases, built on the original TEM studies, although as already noted these newer techniques have yet to make their impact on Al alloys.

TEM characterization of materials is generally broken down into imaging, diffraction and microanalysis, and we will examine the contributions of each of these areas in turn. These areas are not exclusive, since the contrast in the images is often a function of the diffraction pattern and the microanalysis data can also be presented in the form of chemical images. Nevertheless, we will break down the paper into examples of each of these three techniques. The power and

versatility of the TEM lies in the number of signals that are generated from the specimen by a high energy electron beam, all of which can be detected, quantified and in many cases turned into an image of the specimen, as summarized in Figure 1.

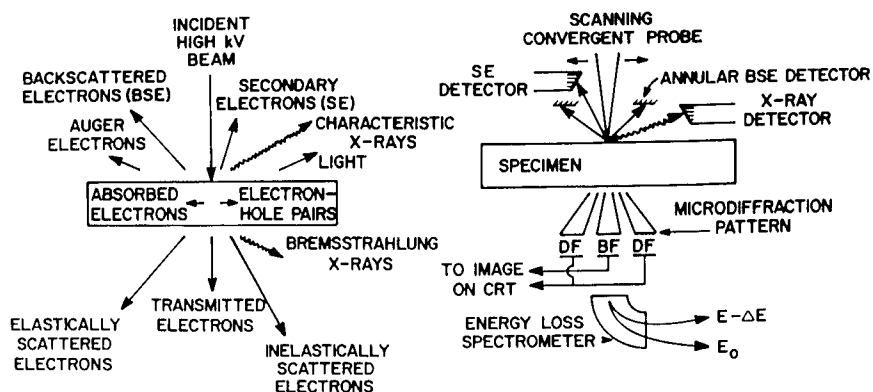


Figure 1. The signals generated in a TEM (left) and the detection systems (right) that permit their translation into quantitative data and images in an analytical scanning TEM. Although all the signals can, in principle, be detected and utilized, in practice TEM images are formed mainly from the transmitted and elastically scattered electrons, and analysis of the chemistry uses the characteristic x-rays and inelastically scattered electrons.

TEM Imaging

Interpretation of images in the TEM is not straightforward. First, the images are always a two dimensional projection of a three dimensional specimen, and this projection can cause problems if it is not taken into account. Second, contrast in the TEM arises for reasons that are not inherently obvious to the eye-brain combination. For example, the principal contrast mechanism for the study of crystalline metals such as Al alloys is diffraction contrast. This mechanism is a function of the diffraction conditions and therefore the contrast changes with changes in specimen tilt and with variations in the specimen orientation, e.g. across interfaces. Interpretation therefore requires an understanding of the phenomenon of diffraction. Nevertheless, direct interpretation of this kind of contrast is extremely valuable because it reveals the presence of defects in the specimen which control the mechanical properties of the materials. The other principal contrast mechanism is phase contrast which is used to reveal the atomic structure of the crystal at the highest magnifications. We will look at examples of both diffraction contrast and phase contrast in Al alloys.

Diffraction Contrast

Diffraction contrast is the standard mode of imaging Al alloys in the TEM. For example, any second phase precipitate that is present in the specimen has either a different structure or a different orientation to the parent Al solid solution matrix. As a result it is a straightforward matter to form images of the second phase precipitate because it diffracts the electrons differently to the matrix. This is shown in Figure 2 [8] which is taken from an Al-Li-Cu specimen in which

the T1 phase has precipitated. The bright field (BF) image (Figure 2a), formed from the transmitted electrons (Figure 1), shows that the bulk of the specimen (i.e. the matrix) is transmitting electrons and the T1 second phase is diffracting them, thus appearing dark. If the electrons diffracted by the precipitate alone are selected to form a dark field (DF) image, then the precipitates appear bright and the matrix is dark (Figure 2b). Note that we only form an image of *some* of the precipitates, since other variants that diffract in different directions are not imaged. Thus DF imaging is very selective, but directly related to the crystallography of the specimen. Since the precipitate-matrix orientation relationship is fundamental to determining the mode of precipitate nucleation (homogenous/heterogeneous) and the state of the interface (coherent, incoherent etc.) DF imaging is a valuable tool. From Figure 2 it is clear that the T1 phase is rod-like rather than the usual plate shape of the T1 phase. Furthermore, it is simple to ascertain that the T1 has nucleated heterogeneously, that the precipitate has a strong orientation relationship to the matrix and therefore the long edge of the precipitate is probably semicoherent with the matrix and the rapidly growing ends are incoherent. These conclusions have obvious relevance to understanding the role of this particular phase in preventing dislocation motion.

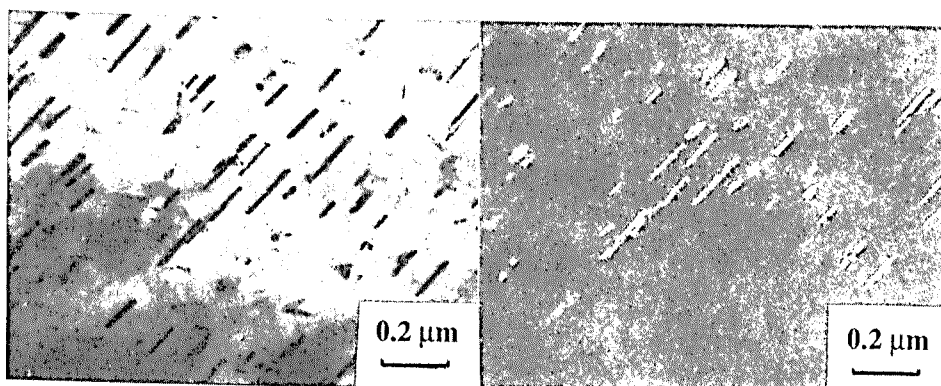


Figure 2. BF, and DF images from an aged Al-Cu-Li alloy showing rod-like T1 precipitates. The BF image (left) reveals all precipitates but in the DF image (right) only one variant is visible (reproduced from [8], courtesy of Pergamon Press).

Simple DF images of precipitates, such as in Figure 2 are valuable because they give a direct measure of the precipitate size, without any complications of strain contrast which occurs in BF images (see below). Direct measure of the precipitate size, with appropriate corrections for sectioning effects of thin foils and careful calibration of the instrument, permit such factors as nucleation rate, growth mechanism and coarsening/dissolution kinetics to be evaluated. All of these have been applied directly to the study of Al alloys at various times. For example, the homogeneous nucleation rate of δ' in Al-Li alloys has been documented [9] along with the direct measurement of the critical nucleus size and the surface energy of the homogeneous precipitates, as summarized in [10]. The vexed question of whether a coherent precipitate forms by nucleation or spinodal decomposition has been addressed for example in Al-Cu alloys [11], Al-Li alloys [12, 13] and Al-Zn alloys - where in fact it proved essential to resort to small angle x-ray scattering rather than TEM to show conclusively the presence of a spinodal [14]. Growth rates of grain boundary θ precipitates were measured and the "collector-plate" growth mechanism devised by Aaron and Aaronson [15]. Lifshitz-Wagner coarsening kinetics invariably require the demonstration of a $t^{1/3}$ dependence of precipitate size and this too has been observed in many Al alloys, with perhaps the most work again been carried out in the Al-Li system e.g. [16, 17].

When imaging in diffraction contrast mode, the coherency state can be directly ascertained because it is also possible to reveal the presence of defects at the interface of any precipitate. Dislocations scatter electrons differently to the perfect crystal and are thus revealed as dark lines in the image as shown in Figure 3. Interpretation of Figure 3 is not straightforward, however. The row of dislocation lines is either piling up at the grain boundary, or being emitted from the boundary. Conclusive discrimination of the two interpretations would require *in-situ* deformation studies in which the motion of the dislocations could be discerned (unless the motion could be induced by beam heating). However, the presence of a precipitate phase at the point on the boundary where the dislocations intersect would seem to indicate that we are viewing a source rather than a pile-up. Such difficulties emphasize one limitation of TEM, while highlighting the clear demonstration of the instrument's abilities to observe crystal defects.



Figure 3. BF image of dislocations emitted from a grain boundary source (courtesy A. K. Vasudevan)

Under certain conditions, dislocations and other defects such as stacking faults, twins and anti-phase boundaries do not diffract and are therefore invisible [18]. But from these invisibility conditions it is possible to deduce the Burgers vector of the dislocation or the displacement vector of the fault. Diffraction contrast therefore results in *quantitative* defect analysis. In addition to determining the Burgers vectors of dislocations, and displacement vectors of faults it is also possible to calculate the axis-angle pair relationships across a grain boundary or interphase interface. In fact, all such planar and line defects can be characterized unambiguously via TEM diffraction contrast and this a unique capability of the instrument, not shared by any other characterization tool [18]. The powerful combination of imaging both the defect and the second phase has meant that the whole question of the interrelationship of boundary structure and the heterogeneous nucleation of precipitates could be attacked. This has seen a wealth of studies, starting in the 1960s [19] and proceeding for the next twenty five years (e.g., [20-23]). All studies of growth have been inextricably linked with the question of the role of ledges in precipitate growth, initially proposed by Laird & Aaronson [24], and now generally accepted as

the standard mechanism by which a semi-coherent interface can migrate while maintaining its favored, faceted orientation relationship with the matrix.

The fine structure of crystal defects can be further revealed by specialized diffraction contrast techniques such as weak beam dark field (WBDF) which permit much finer detail to be revealed as shown in the comparison of images in Figure 4 [23]. In this figure, the grain boundary in an Al-Cu-Ag alloy is imaged in strong diffraction conditions and the dislocations and precipitates at the grain boundary are masked by the strain contrast. In the adjacent WBDF image, the boundary precipitates are revealed as straight lines in the boundary plane and the precipitates in the matrix appear much more clearly defined against the background. The diffraction vector (111) confirms that the precipitates are on the matrix (111) plane.

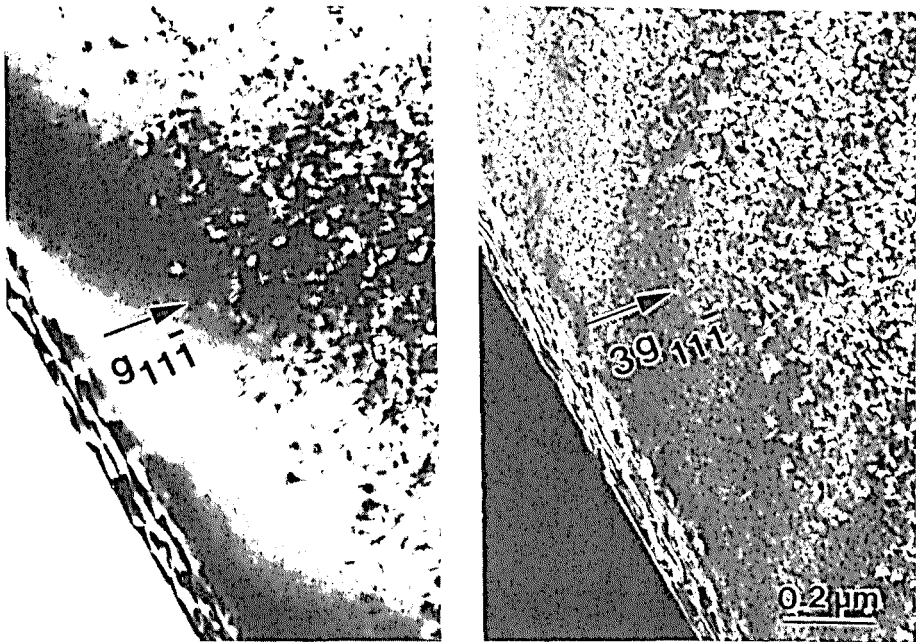


Figure 4. BF and WBDF images of grain boundary and matrix precipitates in a specimen of Al-Cu-Mg-Ag. In the BF image (left) detail of the boundary defect structure on which θ' plates are precipitating and the shape of the matrix precipitates is obscured. These details are revealed in the WBDF image (right) (reproduced from [23], courtesy of Pergamon Press).

This strain contrast which can mask detail in diffraction contrast images such as Figure 4 arises because any lattice strain bends the lattice planes, thus causing changes in the diffraction behavior. Such strain contrast can, in some circumstances, be useful and is best revealed with rather high order diffraction condition. Figure 5 shows the presence of strain fields around coherent precipitates in Al-Li. Again, it is possible to quantify this strain contrast and determine the magnitude and sign of the strain at individual precipitates confined within the thin foil [25, 26]. The strain field is critical to determining whether or not dislocations will cut through, loop or cross slip and no other technique permits this to be both calculated and observed on the same particles. Figure 6a shows dislocation cut through of coherent precipitates in a standard DF image while looping around precipitates is revealed in a WBDF image in Figure 6b.

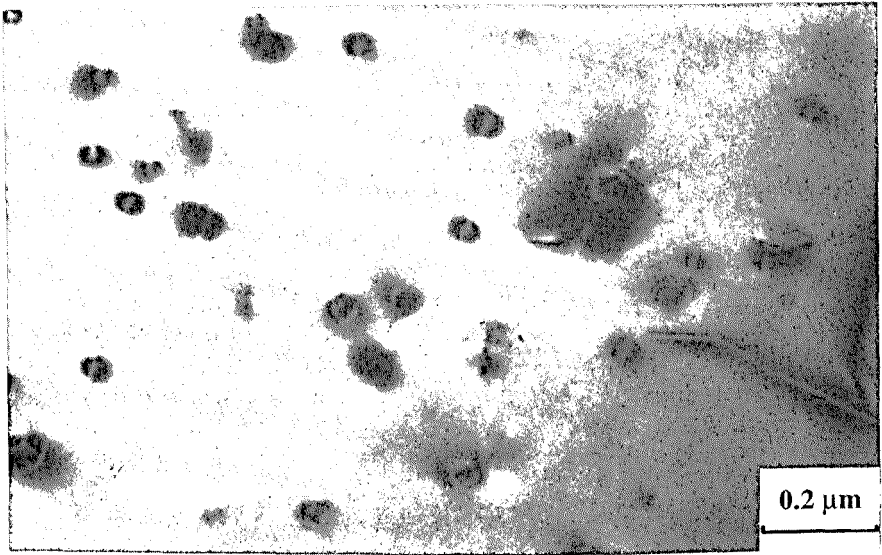


Figure 5. Ashby-Brown strain contrast around small coherent δ' (Al_3Li) precipitates in binary Al-Li alloy, revealed using a high order BF image.

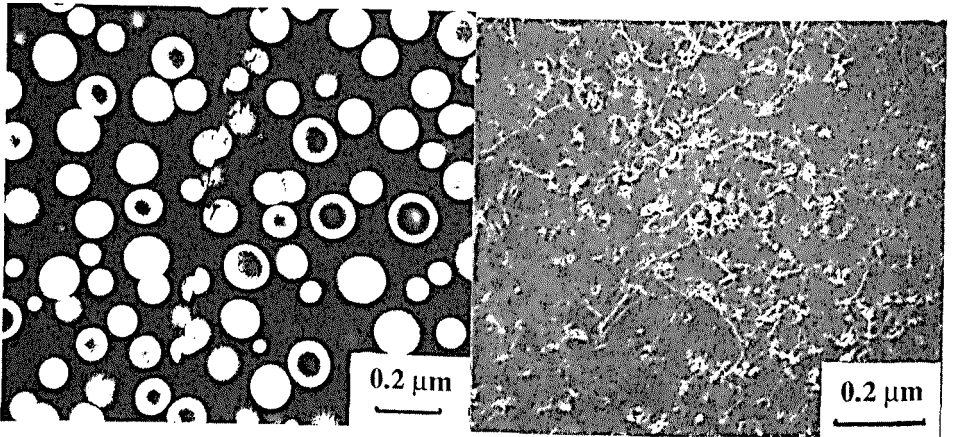


Figure 6a. DF image revealing dislocation cut-through of coherent δ' precipitates b) WBDF image showing dislocation looping around the same precipitates as in 6a, when the coherency strain is increased through ternary Zn alloying additions (Courtesy S. F. Baumann).

The ability to discern dislocation-particle interactions in the TEM is crucial to understanding and predicting the mechanical properties of age-hardened alloys, which constitute a major fraction of commercial Al alloy use. Slip localization as in Figure 6a is thought to contribute to the relatively poor deformation characteristics of Al-Li base alloys. Dispersed slip as in Figure 6b is

more highly desirable, but cannot be obtained in a δ' strengthened alloy alone without unrealistically large alloying additions [26]. Consequently, commercial Al-Li base alloys require other semi-coherent precipitates such as θ' in Al-Li Cu to disperse slip.

Phase Contrast

When the electrons pass through the thin specimen they are scattered by the atoms, e.g. via diffraction from crystal planes as we have seen. The scattered and unscattered electrons, which differ in phase, are recombined rather than separated as in diffraction contrast imaging. This phase difference can be converted into phase contrast, which is the basis of high resolution electron microscopy (HREM). When observed at the highest magnifications ($>500,000\times$) phase contrast images give projected views of either the lattice planes (a so-called lattice image) or a projected view of columns of atoms (structure image). Direct interpretation of either kind of image requires knowledge of the specimen thickness and careful control of the defocus of the microscope objective lens [27]. Full interpretation of the structure images requires a complex calculation of the contrast with an image simulation program, particularly if the structure of defects is to be analyzed [28]. Nevertheless, high resolution phase contrast images are extremely useful when it comes to studying the nature of defects such as grain boundaries or interphase interfaces.

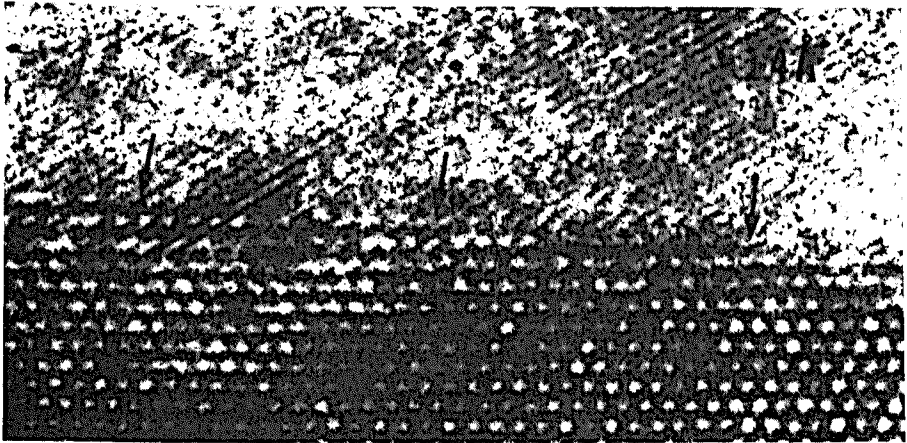


Figure 7. High resolution phase contrast TEM structure image showing the presence of ledges at the interface between a γ' plate in Al-Ag (reproduced from [29], courtesy of Taylor and Francis).

Figure 7 illustrates the power of structure imaging to reveal the complex nature of the precipitate matrix interface in Al-Ag [29]. In this image a series of ledges, each one atom high, is migrating along the precipitate edge. The terraces between the ledges are atomically flat and coherent while the ledges themselves are diffuse and incoherent. Thus growth is accomplished by atomic attachment at the ledges. Similar studies of ledges in Al-Cu precipitates are well known e.g. [30, 31]. In Figure 8, it is shown how a more complex structure, that of Al_3Li (δ') precipitating on θ' in Al-Cu-Li can be interpreted through the aid of simulated phase contrast images [32]. There is reasonable agreement between the contrast in the image and the contrast in the simulation indicating that the proposed atom positions shown schematically on the figure are a valid structure. At this magnification it is straightforward to observe the high degree of coherence between the two precipitate phases since the atomic rows are continuous across the two

interfaces. Similar interpretations have been made of the structure of GP zones [33] illustrating the rapid progress in HREM from the work of Philips already described. While the resolution of microscopes has improved only slightly in the last two decades from ~ 0.3 nm to ~ 0.15 nm, the computer control of the instrument, and the computer calculations of the images have brought increased confidence to both the generation and understanding of these atomic images.

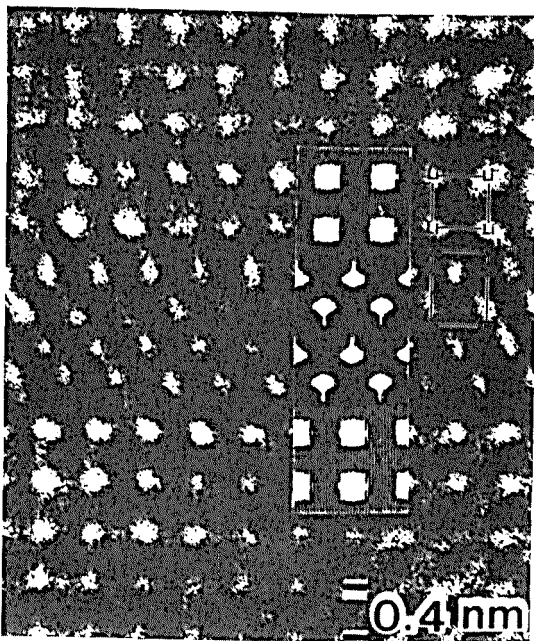


Figure 8. High resolution phase contrast structure image in an Al-Li-Cu alloy showing a thin θ' plate, four atomic planes thick, surrounded by δ' . A computed image is superimposed on the actual image and the proposed positions of the Al, Cu and Li atoms are also indicated. There is a good match between the simulated and experimental images in terms of the atomic positions. (reproduced from [33], courtesy of Taylor and Francis).

Diffraction Patterns

Electron diffraction, which causes the diffraction contrast described above is even more useful in terms of the selected area diffraction (SAD) pattern that is created within the TEM. The SAD patterns offer direct correlation between the crystal structure of the specimen and the TEM image that is formed. This is a major advantage over other diffraction techniques such as x-ray and neutron diffraction which sample relatively large amounts of material, so spatial localization is poor. The classical selected area electron diffraction pattern, such as shown in Figure 9 contains an array of bright spots whose positions represent the spacing of atomic planes in the specimen that lie parallel to the electron beam. From measurements of the spot spacings and angles between the vectors from the central spot to the diffraction spots, the interplanar spacings and angles can be simply determined via Bragg's law [18]. Unfortunately, drawbacks to SAD patterns

are severe. The spatial localization, although better than other diffraction techniques is still relatively poor ($> \sim 1 \mu\text{m}$), the spot intensities arise from multiple dynamical scattering and so are difficult to interpret quantitatively and lattice parameter measurements from the pattern are so inaccurate that unambiguous phase identification is not possible. So SAD patterns are useful only if the specimen is known, in which case the relative orientations of different grains, phases and their defects can be deduced, as illustrated in Figure 9 [8]. From the indexed pattern it is seen that reflection 1 ($10\bar{1}0$) is almost parallel to the $[3\bar{2}1]$ matrix direction, indicating that the T1 habit plane ($10\bar{1}0$) lies on the $(3\bar{2}1)$ matrix plane.

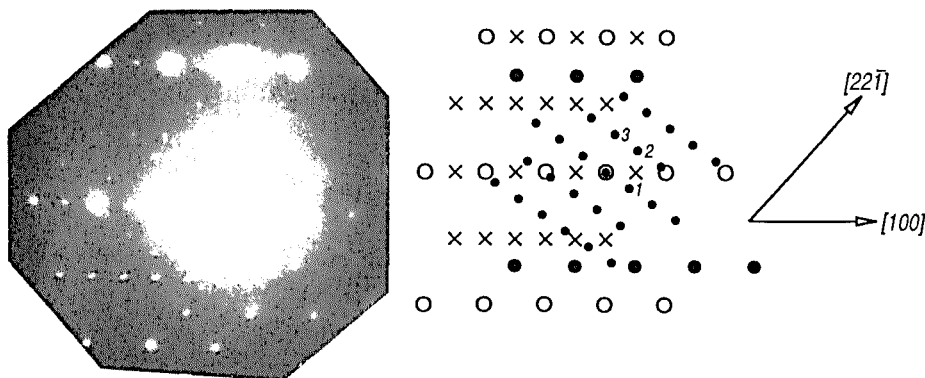


Figure 9. SAD pattern from the region of the Al-Li-Cu alloy shown in Figure 2. The pattern is correctly oriented with respect to the images in Figure 2a and the indexing of the pattern is also shown. The numbered reflections are from the hexagonal T1 phase: 1 = $(10\bar{1}0)$, 2 = $(01\bar{1}2)$ and 3 = $(\bar{1}10\bar{2})$. Two principal matrix crystal directions $[22\bar{1}]$ and $[100]$ are also shown in the schematic diagram (reproduced from [8], courtesy of Pergamon Press).

Such crystallographic analysis of known phases is the principal use of SAD. However, much more information is available in diffraction patterns if the electron beam is focused to a fine probe rather than used as a parallel beam. The diffraction pattern spots then expand to become discs, and within the discs, much new information is available. Such convergent beam electron diffraction (CBED) patterns, are obtainable from very small regions of the specimen, ($< 100 \text{ nm}$) and the detailed contrast within the patterns, as shown in Figure 10, permits lattice parameter measurements, point group and space group determination, thickness measurements, determination of enantiomorphism and a host of other useful crystallographic information [34]. Such 3D crystallographic data is not available in the SAD pattern which contains 2D information only. The upper portion of Figure 10 is a low magnification (camera length) pattern showing high order scatter which contains the 3D structural information, as discussed below. The lower pattern is a reduced exposure of the central portion of the upper pattern revealing similar 3D symmetry information within the discs. Comparison with the SAD pattern in Figure 9 show that the ability of CBED to localize the source of the diffraction to just the precipitate phase provides a much clearer pattern. The wealth of other diffracted intensity is also clear.

Aluminum and its alloys are less well suited to convergent beam diffraction studies than other higher temperature materials. The low melting point of Al means that at ambient temperatures the Debye-Waller factor is such that lattice vibration is significant. The result is that fine detail in the diffraction patterns is washed out. To recover the information it is necessary to cool the specimen, usually close to liquid nitrogen temperatures. An alternative method is to filter out the

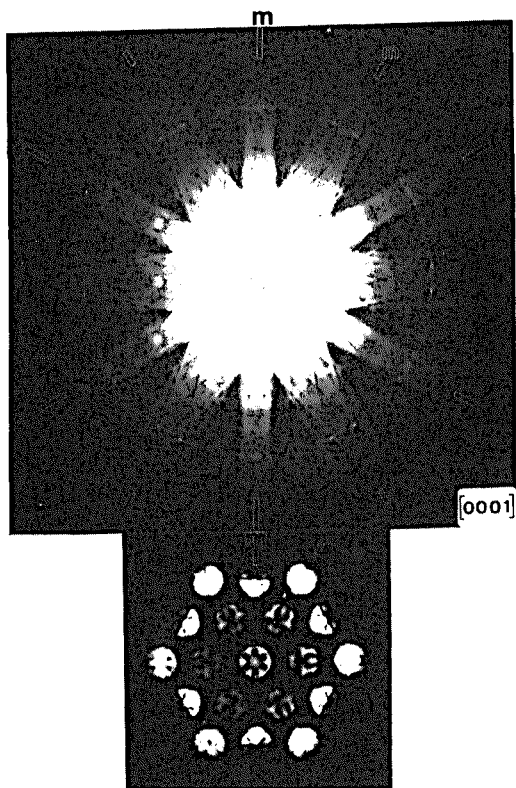


Figure 10. CBED pattern from the hexagonal T1 phase Al_2CuLi . The upper pattern is a low magnification view, and the lower pattern is a higher magnification of the central portion of the upper pattern. The positions of mirror planes (m) in the pattern symmetry are indicated and are useful for point group determination. (reproduced from [34], courtesy of Oxford University Press).

inelastically scattered electrons that are responsible for the high background intensity that swamps the fine detail. Figure 11 illustrates the effect of energy filtering using an electron spectrometer in the column of the TEM to reveal a network of fine lines in the central disc of a CBED pattern of pure Al [35]. These lines are so-called higher-order Laue zone (HOLZ) lines and their symmetry is representative of the full 3D symmetry of the lattice. HOLZ line positions are very sensitive to the lattice parameter of the specimen such that changes as little as 1 part in 10,000 can be deduced. The most powerful aspect of CBED, as already mentioned, is to take all such information and use it to deduce the full 3D symmetry of the crystal. To do this requires taking CBED patterns under varying conditions of magnification, exposure and orientation (as in Figures 10 and 12) and examining the symmetry within the patterns [36, 37], and an example is shown in Figure 12 [38]. Examples of point group determination in addition to that in figure 12 include the Al_3Zr phase [39], T1 in Al-Li-Cu [40] and T2 the icosahedral phase in Al-Li-Cu [41].

In addition to determining the point group it is also possible, with care to find the space group of

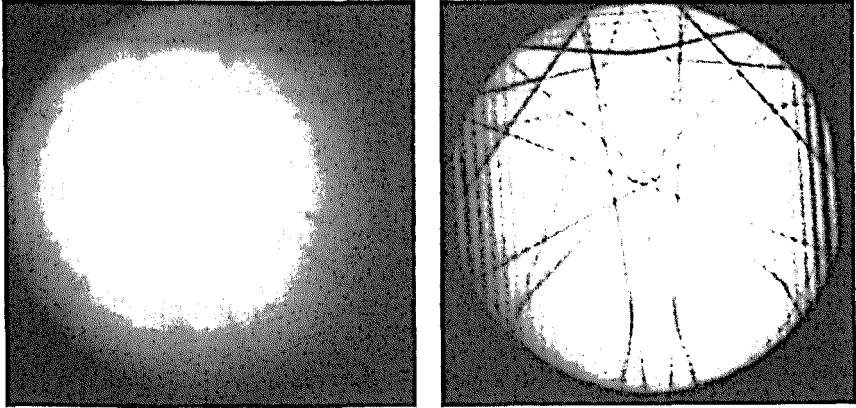


Figure 11. Illustration of how energy-filtering (right) reduces the background noise in a [233] CBED pattern of pure Al cooled to -50°C . The array of HOLZ lines that are almost obscured by the inelastic scattering in the unfiltered (left) pattern are clearly revealed (courtesy J. Mayer).

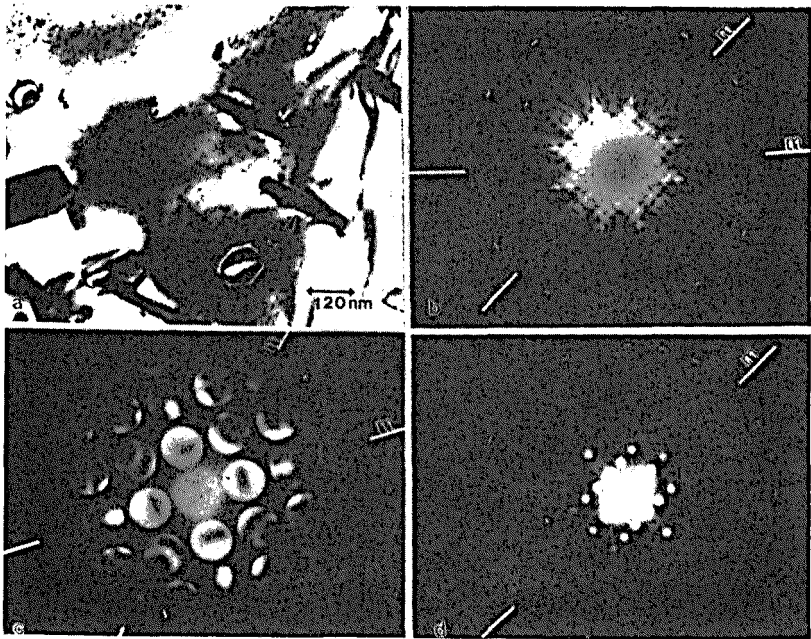


Figure 12. a) BF image showing small Ω precipitates in an Al-Cu-Mg-Ag alloy. The edge-on precipitate arrowed in the image gave rise to the two CBED patterns b), c) used to determine the point group of the second phase. The CBED pattern d) is from the matrix in a [121] orientation (reproduced from [38], courtesy of Pergamon Press).

the phase, the presence or absence of enantiomorphism [34, 36, 37]. Furthermore the specimen thickness can be determined as well as all the standard crystallographic orientation relationships available through SAD patterns. Consequently, CBED is becoming a much more widely used technique for materials characterization, replacing standard x-ray techniques in many cases because of its ability to carry out symmetry determination on phases < 100 nm in size, which do not diffract x-rays with sufficient intensity for crystallographic analysis.

Analytical Electron Microscopy

AEM involves the use of x-ray and/or electron spectrometry in the TEM to acquire quantitative elemental information about the specimen. The electron beam is focused down to a fine probe to localize the source of the spectral information. Therefore the image is lost and so the beam has to be scanned and the signals detected digitally if the image is to be related to the microanalysis. Hence the TEM becomes a scanning TEM (STEM). In Figure 1, it is the characteristic x-rays and the inelastically scattered (energy-loss) electrons that give us quantitative information [42].

X-ray Microanalysis

The idea of quantitative x-ray microanalysis in the TEM is more than 30 years old and the first crude attempts were carried out in the early 1960s. Inefficient x-ray detectors and low intensity thermionic electron sources were severe limitations. Nevertheless valiant attempts were made and by the mid-1970s it was possible to detect sub-micrometer changes in composition, for example across precipitate-free zones, thus revealing for the first time the role of solute-depletion versus vacancy depletion in the creation of these dangerous heterogeneities in the microstructure [6]. It was not until reasonable commercial instruments appeared in the late 1970s that the analytical aspects of TEM really grew. Since then it has become a routine matter to acquire composition profile data such as shown in Figure 13. In this example of quantitative x-ray energy-dispersive spectrometry, an Al-Mn (AA3005) alloy that undergoes accelerated intergranular corrosion has been analyzed. The intensity of the characteristic x-ray peaks of Al and Mn emitted from the thin foil can be related directly to the elemental composition at each point of analysis through a simple equation [42]. The Mn content is shown to be severely

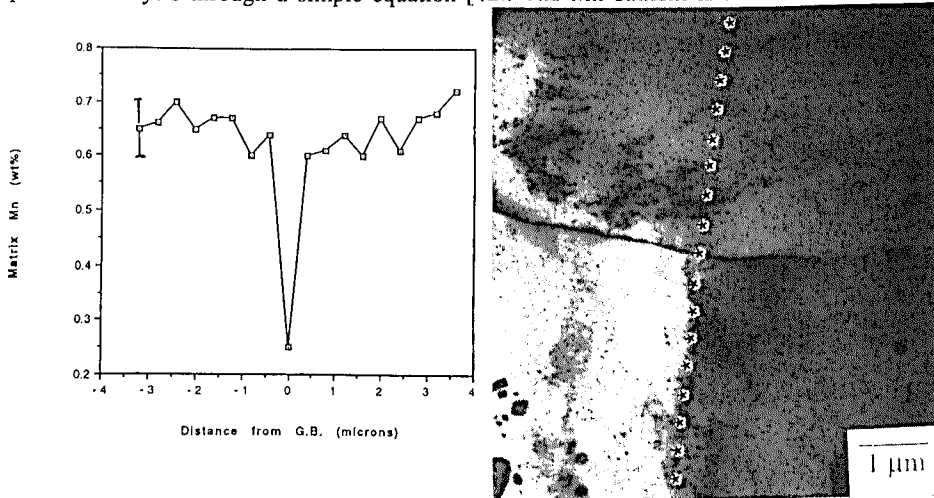


Figure 13. Mn composition profile across a grain boundary in an aged Al-Mn alloy, determined using x-ray microanalysis (courtesy S. F. Baumann).

depleted around the grain boundaries, due to the precipitation of a Mn-rich phases on the boundary. Mn has a strong effect on the corrosion potential of Al and so this depletion is a possible explanation of the susceptibility of the alloy to intergranular corrosion. Similar profiles have been shown to be responsible for precipitate-free zones in Al-Ag [43] and Al-Zn-Mg [44] In Al-Zn [45] the profiles have been used to determine solute diffusion coefficients. Likewise, segregation accompanying aging [46] and precipitation phenomena [47] has been studied using this technique. From the diffusion profile data it is possible to invoke interfacial equilibrium concepts and thence deduce the composition of the ends of the tie lines joining the matrix and precipitate phase fields, thus delineating the solvus lines for phase diagram determination [43].

Electron Energy-loss Spectrometry

Electron energy-loss spectrometry (EELS) is a much more difficult analytical technique than x-ray microanalysis, requiring the creation of very thin specimens, and the analysis of complex spectra. Knowledge of the electronic structure of the elements and the physics of electron-solid interactions is also extremely useful. As a result this technique has been rather sparsely applied to the study of Al alloys. For these reasons there has been little use of the technique, even though it is well suited to the study of the light elements. But in the particular case of Al-Li alloys, EELS is the only technique capable of localizing and detecting Li with high spatial resolution. Consequently there have been many attempts over the years to detect and quantify Li with varying degrees of success. Basically it has proven possible to measure Li diffusion profiles [48] and determine the Al-Li solid solution (α) - Al_3Li (δ') phase field using EELS [49]. The results agree with other indirect approaches such as SAXS, [50] volume fraction determination [51] and x-ray diffraction [51], but were achieved by the direct measurement of the Li content of individual δ' particles. It is possible to examine the EELS spectra to determine the bonding state of the Al and Li elemental constituents (which are metallic in both cases, which is not surprising). However, it is possible to see changes in the fine structure of the Al edge due to, for example oxidation of the Al to Al_2O_3 [52]. The EELS spectrum can also be used to measure local composition changes [53] and it is even possible to distinguish different symmetries of bonding of Al in spinels [54].

Spectra are not the most aesthetic aspect of electron microscopy, especially in comparison with the spectacular high resolution and DF images that are commonly displayed in the metallurgical journals. However, it is possible to convert the spectral information into maps of intensity in which the intensity can be related directly to the amount of the element present. Such maps are described in a separate paper in these proceedings [55] and will not be discussed here.

Summary

The TEM has proven invaluable in elucidating the microstructure and microchemistry of Al-base alloys. Almost all our knowledge of the precipitation behavior of the critical metastable age-hardening phases has been revealed by TEM. This knowledge includes the precipitation formation mechanisms such as nucleation or spinodal decomposition. The mechanisms and kinetics of growth and coarsening have been described. The nature of the dislocation-particle interactions and the coherency state of the interface that together cause precipitation strengthening have been characterized through TEM imaging. CBED can reveal the complete crystallographic aspects of very small precipitates, thus aiding phase diagram determination and an understanding of phase equilibria in general. Analysis in the TEM broadens all the above knowledge because local chemistry changes can also affect the precipitation behavior and the dislocation interactions, as well as promoting stress corrosion and other forms of local failure. As TEM imaging techniques approach the 0.1 nm limit at which almost all metallurgical atomic planes can be resolved and all defects fully analyzed, there will be continued use of the TEM for atomic level engineering. Analysis techniques are also approaching the sub-nanometer resolution level, offering the prospect of detailed chemical probes of bonding at interfaces, which are

42. D. B. Williams, Practical Analytical Electron Microscopy in Materials Science, (Mahwah, NJ, USA: Philips Electron Optics Publishing Group, 1984).
43. S. M. Merchant, M. R. Notis and D. B. Williams, Met. Trans., 14A, (1983) 1825.
44. M. Raghavan, Met. Trans., 11A, (1980) 993.
45. A. W. Nicholls, and I. P. Jones, J. Phys. Chem. Solids, 44, (1983), 671.
46. T. Malis and M. C. Chaturvedi, J. Mater. Sci., 17, (1982), 1479.
47. J. M. Howe, Phil. Mag. Lett., (1994) in press.
48. D. B. Williams and J. W. Edington, Phil. Mag., 30, (1974), 1147.
49. D. R. Liu and D. B. Williams, Proc. Roy. Soc. (London) A, 421, (1989), 91.
50. S. Ceresara, G. Cocco, G. Fagherazzi and L. Schiffini, Phil. Mag., 31, (1977) 373.
51. D. R. Liu and D. B. Williams, Scripta Met., 22, (1988), 1361.
52. D. E. Johnson, S. Csillag and E. A. Stern, Scanning Electron Microscopy, O. Johari, ed., (O'Hare, Chicago, IL, USA: AMF, 1981), 105.
53. M. M. Disko, M. J. Luton and H. Shuman, Ultramicroscopy, 37, (1991), 202.
54. R. Brydson, B. G. Williams, W. Engel, T. Lindner, M. Muhler, R. Schlogl, E. Zeitler and J. M. Thomas, J. Chem. Soc. Faraday Trans., 1, 84, (1988), 631.
55. D. B. Williams, J. A. Hunt and K. K. Soni, these proceedings.